Electronic Structure and Optical Properties of Mixed Phenylene Vinylene/Phenylene Ethynylene Conjugated Oligomers

A. P. H. J. Schenning,[†] A. C. Tsipis,[‡] S. C. J. Meskers,[†] D. Beljonne,[‡] E. W. Meijer,*[,†] and J. L. Brédas*[,‡,§]

Laboratory of Macromolecular and Organic Chemistry, Eindhoven University of Technology, P.O. Box 513, 5600 MB Eindhoven, The Netherlands, Laboratory for Chemistry of Novel Materials, Center for Research on Molecular Electronics and Photonics, University of Mons-Hainaut, Place du Parc 20, B-7000 Mons, Belgium, and Department of Chemistry, The University of Arizona, Tucson, Arizona 85721-0041

Received September 28, 2001. Revised Manuscript Received December 20, 2001

We present a combined experimental and theoretical investigation of the photophysical properties of four π-conjugated oligomers with varying chemical constitutions. Three of these contain alkoxy-substituted *p*-phenylene vinylene/ethynylene units with a phenylene, anthracene, or *p*-dialkoxyphenylene moiety as the central aromatic ring; the fourth oligomer contains only *p*-dialkoxyphenylene vinylene units. The electronic structure and optical properties are investigated by combining UV−vis, fluorescence, and electrochemical techniques with quantum-chemical semiempirical calculations. The simulated absorption spectra are in excellent agreement with the experimental data and illustrate the role of the central aromatic ring on the nature of the lowest excited state.

Introduction

Over the past decade, oligomeric and polymeric organic materials have come into the focus of contemporary materials science for their functional properties and application in optoelectronic devices such as liquid crystal displays (LCDs), field effect transistors (FETs), organic solar cells, and light emitting diodes (LEDs).[1] The main issues in the development of these devices are efficiency and material stability. In LEDs, this efficiency strongly depends on the fluorescence quantum yield of the polymer. Two classes of π-conjugated polymers that have been used as active layers in LEDs are poly(*p*-phenylene vinylene)s (PPV)[2] and poly(*p*-phenylene ethynylene)s (PPE).[3] PPEs have a high fluorescence quantum yield and are considered to be less conjugated than PPVs due to the presence of the carbon−carbon triple bonds.[4] Even though PPEs have not been presented as the most promising emitting layers in LEDs,[5] some efficient devices have been reported.[6] On the other hand, PPVs are among the most extensively studied active layers to be incorporated in polymer-based LEDs that are now at a precommercial stage.

Hybrid conjugated aromatic polymers, having carbon−carbon double and triple bonds, could be of interest because in principle they combine high quantum yields of fluorescence as found for PPE with suitability and stability as found in the case of PPV. Such polymers are, however, rare.[7]

To attain insight into the structural and electronic properties of (polydisperse) polymers, synthesis of corresponding monodisperse conjugated oligomers is very useful.[8] Recently, the synthesis of a number of monofunctional and bifunctional oligo(*p*-phenylene vinylene)s[9] (OPV)s and oligo(*p*-phenylene ethynylene)s[10] (OPE)s

* To whom correspondence should be addressed.
[†] Eindhoven University of Technology.
[‡] University of Mons-Hainaut.
[§] The University of Arizona.

(1) For example, see: (a) Sariciftci, N. S.; Smilowitz, L.; Heeger, A. J.; Wudl, F. *Science* **1992**, *258*, 1474. (b) Yu, G.; Gao, J.; Hummelen, J. C.; Wudl, F.; Heeger, A. J. *Science* **1995**, *270*, 1789. (c) Halls, J. J. M.; Walsh, C. A.; Greenham, N. C.; Marseglia, E. A.; Friend, R. H. *Nature* **1995**, *376*, 498. (d) Ouali, L.; Krasnikov, V. V.; Stalmach, U.; Hadziioannou, G. *Adv. Mater.* **1999**, *11*, 1515. (e) Mitschke, U.; Bäuerle, P. *J. Mater. Chem.* **2000**, *10*, 1471. (f) Brown, A. R.; Pomp, A.; Hart, C. M.; de Leeuw, D. M. *Science* **1995**, *270*, 972. (g) Horowitz, G. *Adv. Mater.* **1998**, *10*, 365. (h) Sirringhaus, H.; Brown, P. J.; Friend, R. H.; Nielsen, M. M.; Bechgaard, K.; Langeveld-Voss, B. M. W.; Spiering, A. J. H.; Janssen, R. A. J.; Meijer, E. W.; Herwig, P.; de Leeuw, D. M. *Nature* **1999**, *401*, 685.

(2) (a) Burroughes, J. H.; Bradley, D. D.; Brown, A. R.; Marks, R. N.; Mackay, K.; Friend, R. H.; Burn, P. L.; Holmes, A. B. *Nature* **1990**, *347*, 539. (b) Braun, D.; Heeger, A. J. *Appl. Phys. Lett.* **1991**, *58*, 1982. (c) Gustafsson, G.; Cao, Y.; Treacy, G. M.; Klavetter, F.; Colaneri, N.; Heeger, A. J. *Nature* **1992**, *357*, 477. (d) Staring, E. G. J.; Demandt, R. C. J. E.; Braun, D.; Rikken, G. L. J.; Kessener, Y. A. R. R.; Venhuizen, A. H. J.; van Knippenberg, M. M. F.; Bouwans, M. *Synth. Met.* **1995**, *71*, 2179.

(3) (a) Swanson, L. S.; Shinar, L.; Ding, Y.; Barton, T. J. *Synth. Met.* **1993**, *55*−*57*, 1. (b) Weder, C.; Wagner, M. J.; Wrighton, M. S. *Mater. Res. Soc. Symp. Proc.* **1996**, *413*, 77.

(4) Swager, T. M.; Gil, C. J.; Wrighton, M. S. *J. Phys. Chem.* **1995**, *99*, 4886.

(5) Kraft, A.; Grimsdale, A. C.; Holmes, A. B. *Angew. Chem., Int. Ed.* **1998** *37*, 402.

(6) Montali, A.; Smith, P.; Weder, C. *Synth. Met.* **1998**, *97*, 123.

(7) (a) Jeglinski, S. A.; Amir, A.; Wei, X.; Vardeny, Z. V.; Shinar, J.; Cerkvenik, T.; Chen, W.; Barton, T. J. *Appl. Phys. Lett.* **1995**, *67*, 3960. (b) Brizius, G.; Pschirer, N. G.; Steffen, W.; Stizer, K.; zur Loye, H.-C.; Bunz, U. H. F. *J. Am. Chem. Soc.* **2000**, *122*, 12435. (c) Ramos, A. M.; Rispens, M. T.; van Duren, J. K. J.; Hummelen, J. C.; Janssen, R. A. J. *J. Am. Chem. Soc.* **2001**, *123*, 6714. (d) Egbe, D. A. M.; Tillmann, H.; Birckner, E.; Klemm, E. *Macromol. Chem. Phys.* **2001**, *202*, 2712.

(8) *Electronic Materials: The Oligomeric Approach*; Wegner, G., Mullen, K., Eds.; Wiley-VCH: Weinheim, 1998.

10.1021/cm0109185 CCC: $22.00
Published on Web 02/21/2002

Scheme 1

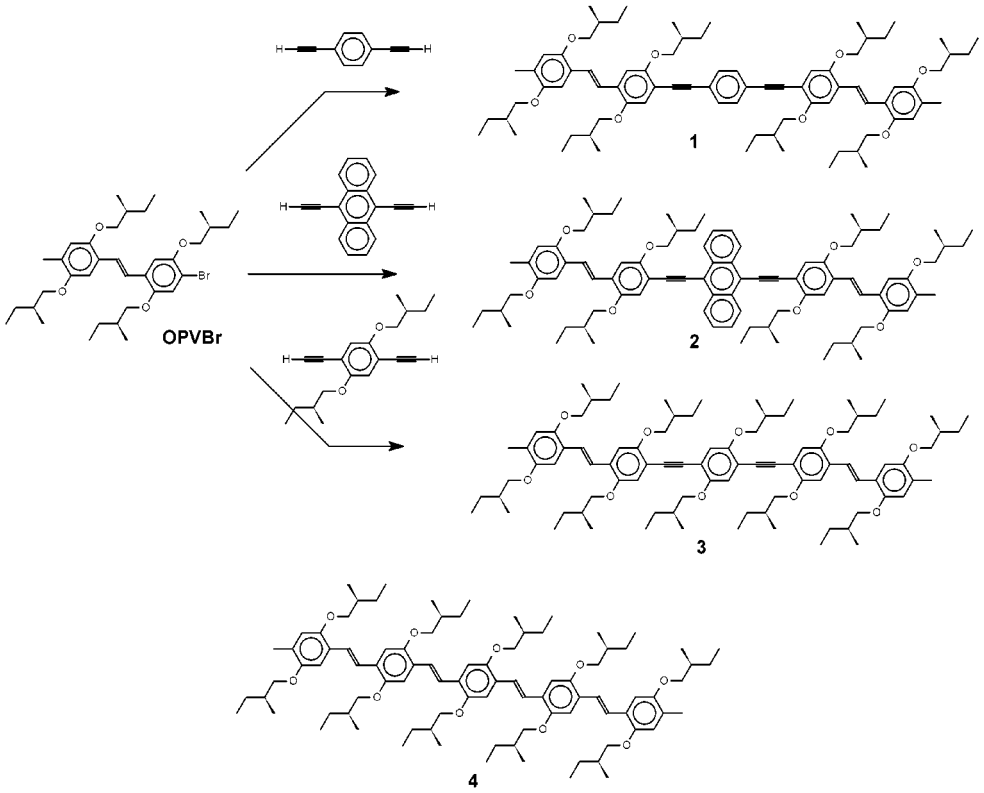

has been reported. Here, we discuss a comprehensive theoretical and experimental study on π-conjugated oligomers combining double and triple bonds (Scheme 1).

Results and Discussion

Synthesis. Oligomers **1**−**3** were synthesized via a palladium cross-coupling reaction of **OPVBr** with the diethynylenearene units (Scheme 1).[11] In all cases, the yields were higher then 80%. The compounds were fully characterized with NMR, IR, mass spectroscopy, and elemental analysis. The IR spectra of the oligomers displayed the typical C≡C vibration at about 2200 cm^{-1}. Pentamer **4** that only contains double bonds acts as a model compound for the corresponding PPV polymers; its synthesis has been published elsewhere (Scheme 1).[12]

An interesting phenomenon was observed when **3** was heated above the melting point (220 °C) and then slowly cooled under a polarization microscope (Figure 1). During crystallization, fibers were formed that present alternating black and white bars when circularly polarized light was used. Depending on the direction of the polarized light, mirror images were obtained. The origin of this phenomenon is currently under investigation.

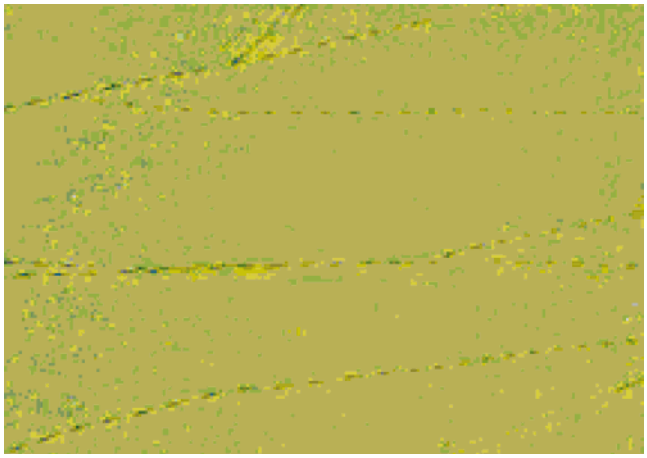

Figure 1. Polarization microscope photograph of **3** at 190 °C obtained after heating above the melting temperature and then slowly cooling.

Optical Properties. The optical absorption spectra of **1**−**4** were measured in dichloromethane; they are given in Figure 2 with the physical characteristics detailed in Table 1. As can be seen from the Figure, the absorption maximum shifts to the red in the following order: **1**−**3**−**4**−**2**. This sequence can be understood on the basis of the different natures of the central units in the four oligomers, as described in the theoretical section.

The fluorescence spectra of the oligomers are reported in Figure 3, while the emission maxima are listed in Table 2. The emission maximum shifts to the red in the same sequence as that found for the absorption maximum. The fluorescence peaks of **1** and **3** are narrower than found for **2** and **4**. The fluorescence quantum yield is the highest in the case of **1**.

(9) For examples, see: (a) Maddux, T.; Li, W.; Yu, L. *J. Am. Chem. Soc.* **1997**, *119*, 844. (b) Stalmach, U.; Kolshorn, H.; Brehm, I.; Meier, H. *Liebigs Ann.* **1996**, 1449. (c) Schenk, R.; Gregorius, H.; Meerholz, K.; Heinze, J.; Mullen, K. *J. Am. Chem. Soc.* **1991**, *113*, 2634. (d) Drefahl, G.; Plotner *Chem. Ber.* **1958**, *91*, 1274.

(10) For example, see: (a) Zhang, J.; Moore, J. S.; Xu, Z. F.; Aguirre, R. A. *J. Am. Chem. Soc.* **1992**, *114*, 2273. (b) Jones, L.; Schumm, J. S.; Tour, J. M. *J. Org. Chem.* **1997**, *62*, 1388. (c) Lavastre, O.; Ollivier, L.; Dixneuf, P. H.; Sibandhit, S. *Tetrahedron* **1996**, *52*, 5495.

(11) Takahashi, S.; Kuroyama, Y.; Sonogashira, K.; Hagihara, N. *Synthesis* **1980**, 627.

(12) Peeters, E.; Marcos, A.; Meskers, S. C. J.; Janssen, R. A. J. *J. Chem. Phys.* **2000**, *112*, 9445.

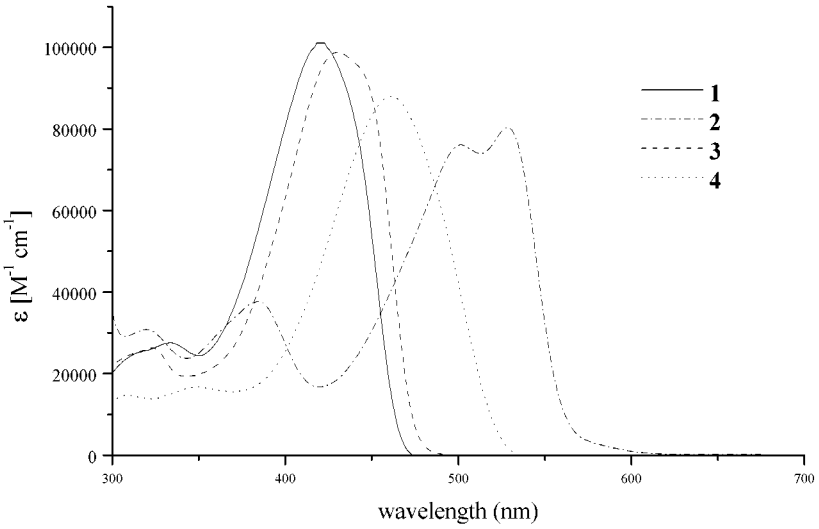

Figure 2. UV-vis spectra of **1**−**4** in dichloromethane.

Table 1. Absorption Data of 1−4

	absorption[a] λ_{max} (nm)	log ϵ	absorption[b] λ_{max} (nm)	O. S.[c] (a.u.)	CI[d]
1	415	5.00	381	3.74	0.81HL + 0.48H-1 L + 1
2	523	4.90	461	2.37	0.94HL + 0.23H-1 L + 1
3	426	4.99	387	3.64	−0.82HL −0.45H-1 L + 1 + 0.24H - 2L + 2
4	454	4.94	410	3.35	−0.85HL −0.39H-1 L + 1

[a] Measured in dichloromethane. [b] Calculated from INDO/SCI simulated absorption spectra of the planar conformers. [c] Calculated oscillator strength of the lowest optically allowed transition of the planar conformers. [d] CI coefficients of the planar conformers.

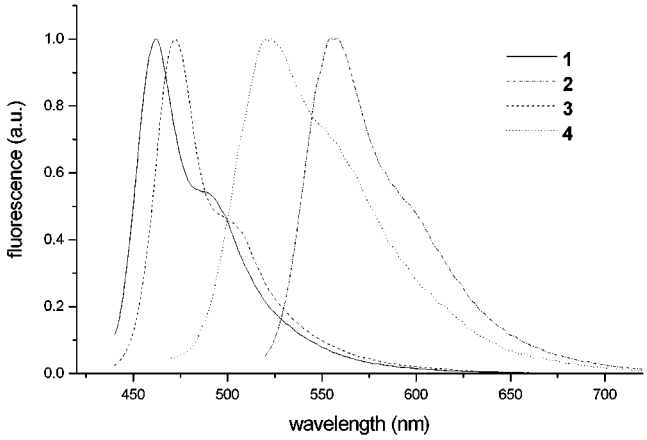

Figure 3. Fluorescence spectra of **1**−**4** in dichloromethane.

The lifetime of the singlet excited state (τ) has been determined using single photon counting time-resolved photoluminescence.[12] The decay curves have been fitted with a single-exponential decay. The time constants are listed in Table 2 and reveal a reduction of the excited-state lifetime in the following sequence: **2**−**1**−**3**−**4**. From the fluorescence quantum yields and τ, the radiative (k_r) and nonradiative (k_{nr}) rate constants were calculated (Table 2).[12]

The lowest energy absorption band and the fluorescence of **2** are remarkably red-shifted with respect to **1** and **3**. The spectral data may be compared to those reported for (9,10)bis(phenylethynyl)anthracene.[13] The absorption maximum of this compound lies at 455 nm ($\epsilon = 33 \times 10^3$ $M^{-1}cm^{-1}$). The wavelength of maximum

Table 2. Fluorescence Data of 1−4

	fluorescence λ_{max} (nm)[a]	ϕn	τ[b] (ns)	k_r (10^8)[c] (s^{-1})	k_{nr} (10^8)[c] (s^{-1})
1	462	0.84	1.3	6.3	1.2
2	556	0.21	2.1	1.0	3.7
3	472	0.69	1.3	5.3	2.4
4	523	0.49	0.9	5.4	5.6

[a] Measured in dichloromethane. [b] Singlet state lifetime. [c] Radiative (k_r) and nonradiative (k_{nr}) decay constants.

emission intensity is at 475 nm with a second vibronic band at 510 nm, and the fluorescence lifetime amounts to 5.5 ns (quantum yield close to unity). The spectral data of **2** show that the S_1 state is considerably lower in energy than that for (9,10)bis(phenylethynyl)anthracene, indicating that the excited state is not localized solely on the phenylethynylanthracene unit. This is also supported by the higher extinction coefficient of **2**.

The luminescence properties of **2** were further investigated in a microcrystalline film, which was prepared by melting the powder between sapphire plates under an inert atmosphere. At low temperature (10 K), the fluorescence showed a time dependent red-shift (Figure 4), characteristic of disordered molecular solids. Shortly after excitation, the luminescence peaks at 670 nm, while in the time window from 2 to 6 ns after excitation, the maximum is shifted to 690 nm. Such a time dependent shift is commonly observed for π-conjugated materials in solid, aggregated form and is usually interpreted in terms of relaxation of the excitation by diffusion to molecular sites with low excitation energy. The decay of the luminescence from the solid film is nonexponential (Figure 5) and shows a rapid decay component on the red side of the fluorescence. The relative contribution of the rapid component was found to depend on excitation density, indicating that this decay is due to exciton−exciton annihilation. This in turn implies that the photoexcitations are rather mobile and diffuse over considerable distances before encountering a second excitation. At longer emission wavelength (690 nm), the contribution from the bi-exciton decay seems to be further reduced, which could be

(13) Berlman, I. B. *Handbook of fluorescence spectra of aromatic compounds*, 2nd ed.; Academic Press: New York, 1971.

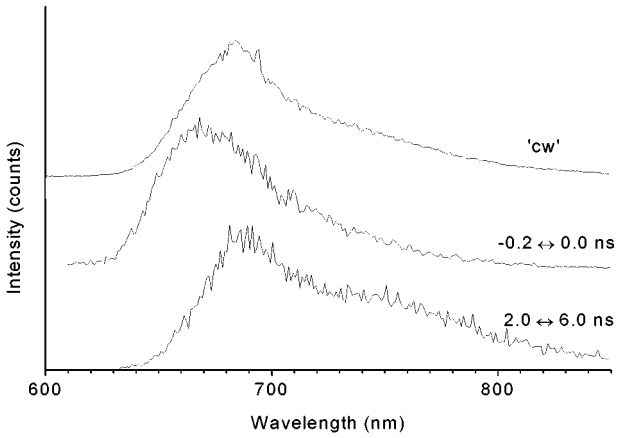

Figure 4. Time integrated ('cw') and time-resolved (time window for data acquisition indicated) fluorescence spectra of **2** at low temperature (10 K).

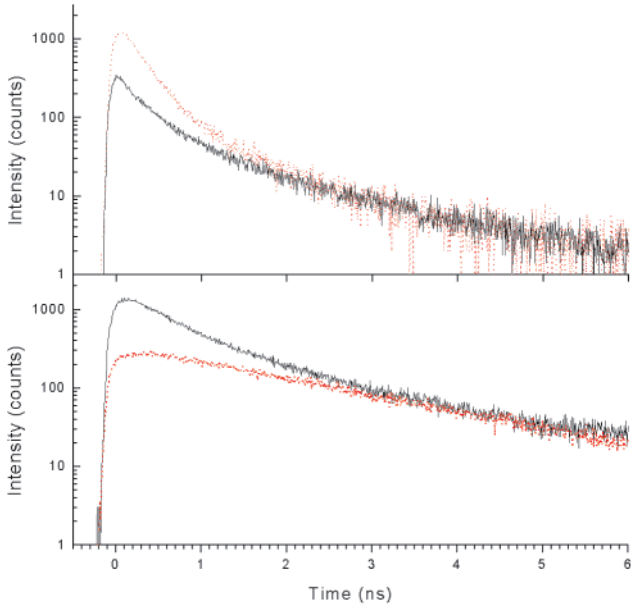

Figure 5. Decay of the fluorescence from **2** at low temperature (10 K, $\lambda_{ex} = 590$ nm). Top figure: dotted line, excitation density = 37nJ/cm^2, $\lambda_{em} = 650$ nm; solid line, excitation density = 6nJ/cm^2, $\lambda_{em} = 650$ nm. Bottom figure: solid line, excitation density = 6nJ/cm^2, $\lambda_{em} = 690$ nm; dotted line, decay in CH_2Cl_2 solution at room temperature.

related to a lower mobility of the relaxed and therefore trapped excitations. Interestingly, the long-lived component in the luminescence has a lifetime that is very close to that observed in solution. The considerable red-shift (0.36 eV) of the luminescence, when comparing solution and solid film, may have several origins. One possibility is a more planar conformation of the molecule resulting in extended conjugation, however, theoretical calculation reveals that the excitation is localized at the anthracene moiety. In addition, intermolecular interactions can contribute to the red-shift, through delocalization of the excitation over several molecules.

Electrochemical Properties. Oxidation and reduction potentials give information on the relative positions of the HOMO (highest occupied molecular orbital) and LUMO (lowest unoccupied molecular orbital). The redox properties of the oligomers were investigated by cyclic voltammetry (CV) in CH_2Cl_2 with Bu_4NPF_6 as ground electrolyte. The results are summarized in Table 3. All

Table 3. Redox Properties of 1−4

	E_{ox1}[a] (V)	E_{ox2}[a] (V)	E_{ox3}[a] (V)	E_{ox4}[a] (V)	E_{HOMO}[b] (eV)	E_{LUMO}[b] (eV)
1	0.95	0.98	1.27	1.29	−6.74	−0.58
2	0.84	0.97	1.17	1.34	−6.32	−0.97
3	0.93	0.97	1.20	1.41	−6.60	−0.56
4	0.73	0.80	1.13	1.30	−6.59	−0.67

[a] Cyclic voltammetry conditions: dichloromethane, 0.1 M Bu_4NPF_6, SCE, and 100 mV/s. [b] INDO-calculated HOMO and LUMO of the planar conformers.

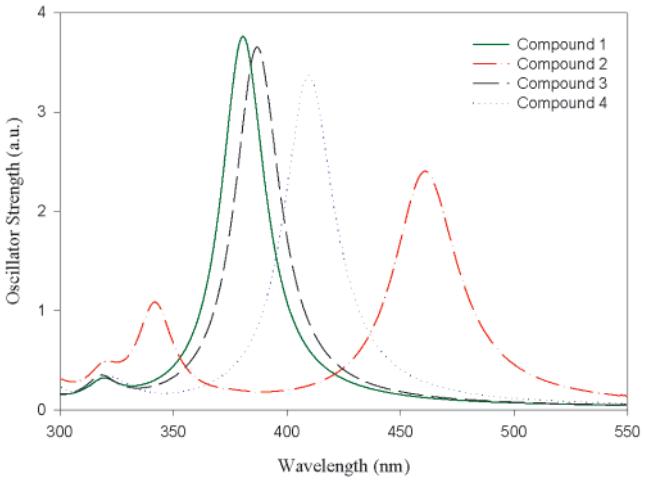

Figure 6. INDO/SCI simulated absorption spectra of planar **1**−**4** conformers. The spectra were convoluted by means of Gaussian functions, with full width at half-maximum set to 0.1 eV.

compounds can be reversibly oxidized to the tetracation state. In the case of **2** also, an irreversible reduction wave was found at −1.51 V. A gap of 2.34 V could be calculated for **2** from the onset of the first reduction and oxidation potentials. This is in good agreement with the optically determined band gap of 523 nm (2.37 eV). Compound **4** has the lowest oxidation potential (0.73 V) followed by **2**, **3**, and **1**.

Theoretical Results. The geometries of all compounds have been optimized at the Hartree−Fock semiempirical Austin model 1 (AM1)[14] level assuming planar conformations. Note that full geometry optimizations yield slightly twisted structures, but we checked that it does not affect the overall picture described below. Since here the focus is on explaining the trends in the optical properties with the nature of the conjugated bridge, it suffices to discuss the case of fully planar conformers.

On the basis of these geometries, the optical absorption spectra of the four oligomers were simulated by combining the INDO Hamiltonian[15] to a single configuration interaction scheme. All singly excited Slater determinants built by promotion of one electron from an occupied π level to an empty π^* level are taken into account. The Mataga−Nishimoto potential[16] has been adopted for the electron−electron interactions, which best reproduces the absorption spectra within the INDO/SCI formalism.

(14) Dewar, M. J. S.; Zoebisch, E. G.; Healy, E. F.; Stewart, J. J. P. *J. Am. Chem. Soc.* **1985**, *107*, 3902.
(15) Ridley, J.; Zerner, M. C. *Theor. Chim. Acta* **1973**, *32*, 111.
(16) Mataga, N.; Nishimoto, K. *Z. Phys. Chem.* (*Munich*) **1957**, *13*, 140.

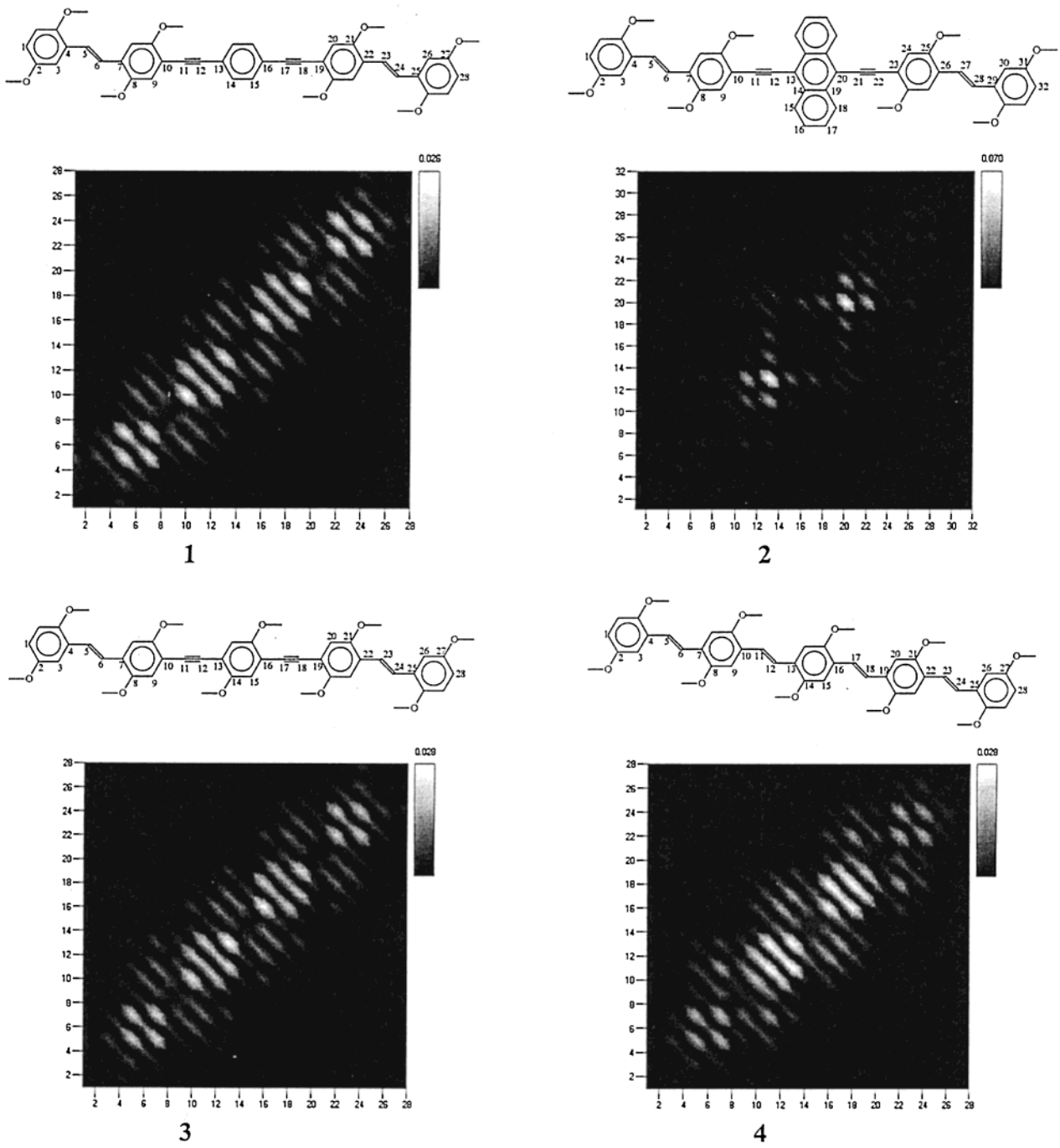

Figure 7. INDO/SCI contour plots of the first excited-state wave functions calculated for **1**−**4** planar conformers (the site labeling is shown on top).

The computed spectra, displayed in Figure 6, are in good agreement with the measured ones. Especially, the first optical transition is calculated to shift to the red in the same sequence as that found experimentally (i.e., **1**−**3**−**4**−**2**). The red shift observed when going from **1** to **3** is due to the electroactive effects induced by the alkoxy groups grafted on the central phenylene ring of **3**; these lead to an asymmetric destabilization of the HOMO and LUMO levels (the HOMO being more affected) and a subsequent decrease in the HOMO−LUMO gap. Compared to **3**, compound **4** is characterized by a further bathochromic shift, which arises from the increased conjugation associated to switching from triple bonds to double bonds around the central unit. Finally, **2** has the lowest optical gap owing to the replacement of the inner phenylene ring with an anthracene moiety; note that this change in absorption maximum stems both from a topological effect (anthracene has a lower optical gap than benzene) and a slightly increased π-delocalization along the chain axis (vide infra).

To analyze the amount of excited-state delocalization in the four molecules investigated, the two-particle electron−hole wave functions have been computed for the lowest singlet excited state at the INDO/SCI level, see Figure 7. These two-dimensional grids run along each axis over all the atoms labeled in the chemical sketch on top of each diagram; each data point (x_i,y_j)

corresponds to the density of probability $|\psi(x_i,y_j)|$ for finding the electron on site x_i and the hole on site y_j

$$\psi(x_i,y_j) = 1/\sqrt{2}[\sum_r C_r^{CI} C_{x_i}^{LCAO}(e^-) C_{y_j}^{LCAO}(h^+) + \sum_j C_r^{CI} C_{x_i}^{LCAO}(h^+) C_{y_j}^{LCAO}(e^-)]$$

where $C_{x_1}(h^+)$ and $C_{x_1}(e^-)$ are the LCAO coefficients in the occupied and unoccupied levels, respectively, that are involved in the *r*th singly excited configuration (with C_r^{CI} being the associated CI coefficient). The bright regions of the graph correspond to the highest probability for finding the particles at these positions.

In all cases, the excited states leading to the first absorption peak have their origin in a transition from a delocalized occupied orbital to a delocalized unoccupied orbital and so the electron and the hole should be spatially overlapped.[17] The bright regions are indeed located along the diagonal and spread out over the whole molecule, except however for **2**. In the latter compound, the wave function is found to be somewhat squeezed on the central part of the molecule, which results from the low ionization potential and high electron affinity of anthracene (hence, the HOMO and LUMO levels involved in the first optical transition have large weights on the anthracene moiety). However, contributions from the chain ends to the wave function albeit small are non-negligible and lead to a red shift in the position of the first optical transition in **2** as compared to (9,10)bis(phenylethynyl)anthracene (this red shift is calculated to be ~0.15 eV and amounts to ~0.35 eV experimentally).

Conclusions

In conclusion, novel π-conjugated oligomers have been synthesized whose optical properties can be tuned by introducing phenylene vinylene or ethynylene units. This holds promise that in the polymers of this type, the energy of the lowest excited singlet state can easily be engineered.

Experimental Section

General Methods. ^{1}H NMR and ^{13}C NMR spectra were recorded on a Varian Gemini 300 or 400 MHz spectrometer, at room temperature. Chemical shifts are given in ppm downfield from tetramethylsilane. Abbreviations used are s = singlet, d = doublet, t = triplet, m = multiplet, and b = broad. IR spectra were obtained with a Perkin-Elmer spectrometer. UV−vis spectra and fluorescence spectra were recorded on a Perkin-Elmer Lambda 40 spectrometer and a Perkin-Elmer luminescence spectrometer LS 50 B in. The melting points were determined using a Jenaval polarization microscope equipped with a Linkam THMS 600 heating device. Elemental analysis was performed on a Perkin-Elmer 2400 series analyzer. Cyclic voltammograms were obtained in dichloromethane with 0.1 M tetrabutylammonium hexafluorophosphate as supporting electrolyte using a Potentioscan Wenking POS73 potentiostat. A platinum disk (diameter 5 mm) was used as working electrode; the counter electrode was a platinum plate (5 × 5 mm^2), and a saturated calomel electrode (SCE) was used as reference electrode. ESI-MS spectra were recorded on a API 300 MS/MS mass spectrometer (PE-Sciex). MALDI-TOF spectra were measured on a Perseptive DE Voyager MALDI-TOF spectrometer utilizing α-cyano-4-hydroxycinnamic acid matrix.

Materials. Commercial grade reagents were used without further purification. All solvents used were p.a. quality. Diethynylbenzene,[11] diethynylanthracene,[18] 1,4-diethynyl-2,5-bis[(2S)-2-methylbutoxy]benzene,[19] and **OPVBr**[20] were synthesized according to literature procedures. Degassing of solvents was accomplished by bubbling argon through the solvent for at least 30 min.

1: A degassed solution of 200 mg (0.324 mmol) of **OPVBr**, 20 mg (0.162 mmol) of diethynylbenzene, 5.4 mg of $PdCl_2$, 26.2 mg of $P(Ph)_3$, and 6 mg of $Cu(OAc)_2$ in 25 mL of Et_3N was stirred at 80 °C under argon atmosphere. After 18 h, the solvent was removed in vacuo. The residue was dissolved in minimal amount of CH_2Cl_2 and passed through a plug of silica. Evaporation of the solvent yielded the crude reaction mixture, which was purified by column chromatography (pentane/CH_2Cl_2, 1:1, v/v) affording **1** as a yellow solid. Mp 145 °C. ^{1}H NMR ($CDCl_3$): δ 0.9−1.1 (m, 48H, CCH_3), 1.2−1.4 (m, 8H, CHH), 1.5−1.7 (m, 8H, CHH), 1.8−2.0 (m, 8H, CH), 2.24 (s, 6H, ArCH_3), 3.7−4.0 (m, 16H, OCH_2), 6.74 (s, 2H, CH_3ArH), 7.01 (s, 2H, CH_3ArH), 7.09 (s, 2H, ≡CArHCH═), 7.18 (s, 2H, ≡CArHCH═), 7.43 (d, 2H, ArCH═CH, J = 16.7 Hz), 7.50 (C≡CArHC≡C), 7.54 (d, 2H, ArCH═CH, J = 16.7 Hz). ^{13}C NMR ($CDCl_3$): δ 11.37, 11.42, 11.47, 16.44, 16.65, 16.69, 16.78, 26.23, 26.34, 34.95, 35.01, 35,09, 73.66 (OCH_2), 74.26 (OCH_2), 74.64 (OCH_2), 88.47 (C≡C), 93.90 (C≡C), 108.40, 109.42, 110.91, 116.23, 116.27, 117.06, 121.37, 123.32, 124.26, 124.86, 127.94, 129.17, 131.30, 150.27 (COCH$_2$), 150.55 (COCH$_2$), 152.65(COCH$_2$), 154.02 (COCH$_2$). IR (KBr): ν (cm^{-1}) = 2958.8 (C−H sat), 2917.1 (C−H sat), 2872.9 (C−H sat), 2203.0 (C≡C). UV−vis (CH_2Cl_2): λ_{max} (ϵ) = 323 (35 000), 415 nm (101 000). ES MS: 1200.0 [M + H$^+$]. Anal. Calcd for $C_{80}H_{110}O_8$: C, 80.09; H, 9.24. Found: C, 80.03; H, 9.37.

2: A degassed solution of 200 mg (0.324 mmol) of **OPVBr**, 37 mg (0.162 mmol) of diethynylanthracene, 4 mg of Pd-$(P(Ph)_3)_2Cl_2$, and 1 mg of CuI in 25 mL of Et_3N was stirred at 80 °C under argon atmosphere. After 18 h, the solvent was removed in vacuo. The residue was dissolved in minimal amount of CH_2Cl_2 and passed through a plug of silica. Evaporation of the solvent yielded the crude reaction mixture, which was purified by column chromatography (pentane/CH_2Cl_2, 3:1, v/v) affording **1** as a yellow solid. Mp 182 °C. ^{1}H NMR ($CDCl_3$): δ 0.9−1.2 (m, 48H, CCH_3), 1.3−1.5 (m, 8H, CHH), 1.5−1.8 (m, 8H, CHH), 1.8−2.0 (m, 6H, CH), 2.1−2.3 (m, 2H, CH), 2.27 (s, 6H, ArCH_3), 3.7−4.1 (m, 16H, OCH_2), 6.77 (s, 2H, ArH), 7.14 (s, 2H, ArH), 7.27 (s, 2H, ArH), 7.28 (s, 2H, ArH), 7.50 (d, 2H, ArCH═CH, J = 16.7 Hz), 7.60 (d, 2H, ArCH═CH, J = 16.7 Hz)) 7.65 (q, 4H, ArH) 8.86 (q, 4H, ArH). ^{13}C NMR ($CDCl_3$): δ 11.36, 11.49, 11.54, 16.44, 16.70, 16.83, 26.23, 26.37, 34.95, 35.03, 35.12, 73.36 (OCH_2), 74.06 (OCH_2), 74.56 (OCH_2), 74.63 (OCH_2), 91.61 (C≡C), 99.98 (C≡C), 108.30, 108.48, 111.95, 116.24, 116.30, 117.27, 118.81, 121.37, 124.25, 124.85, 126.46, 128.00, 129.44, 132.00, 150.26 (COCH$_2$), 150.56 (COCH$_2$), 151.68 (COCH$_2$), 154.58 (COCH$_2$). IR (KBr): ν (cm^{-1}) = 2959.2 (C−H sat), 2917.1 (C−H sat), 2873.9 (C−H sat), 2185.3 (C≡C). UV−vis (CH_2Cl_2): λ_{max} (ϵ) = 380 (40 000), 496 (76 000), 525 nm (80 000). ES MS: 1300.8 [M + H$^+$]. Anal. Calcd for $C_{88}H_{114}O_8$: C, 81.31; H, 8.84. Found: C, 81.05; H, 8.93.

3: A degassed solution of 300 mg (0.324 mmol) of **OPVBr**, 67 mg (0.162 mmol) of diethynyldialkoxybenzene, 7 mg of $PdCl_2$, 36 mg of $P(Ph)_3$, and 8 mg of $Cu(OAc)_2$ in 25 mL Et_3N was stirred at 80 °C under argon atmosphere. After 18 h, the solvent was removed in vacuo. The residue was dissolved in minimal amount of CH_2Cl_2 and passed through a plug of silica. Evaporation of the solvent yielded the crude reaction mixture, which was purified by column chromatography (pentane/CH_2Cl_2, 1:1, v/v) affording **1** as a yellow solid. Mp 212 °C. ^{1}H

(17) Köhler, A.; Santos, D. A.; Beljonne, D.; Shuai, Z.; Brédas, J. L.; Holmes, A. B.; Müllen, K.; Friend, R. H. *Nature* **1998**, *392*, 903.

(18) Scott, L. T.; Necula, A. *Tetrahedron Lett.* **1997**, *38*, 1877.

(19) Fiesel, R.; Scherf, U. *Macromol. Rapid Commun.* **1998**, *19*, 427.

(20) Peeters, E.; van Hal, P. A.; Knol, J.; Brabec, C. J.; Sariciftci, N. S.; Hummelen, J. C.; Janssen, R. A. J. *J. Phys. Chem. B.* **2000**, *104*, 10174.

NMR ($CDCl_3$): δ 0.9−1.1 (m, 60H, CCH_3), 1.2−1.4 (m, 10H, CHH), 1.5−1.7 (m, 10H, CHH), 1.8−2.0 (m, 10H, CH), 2.27 (s, 6H, ArCH_3), 3.7−4.0 (m, 20H, OCH_2), 6.76 (s, 2H, CH_3ArH), 7.03 (s, 4H, CH_3ArH), 7.13 (s, 2H, ArH), 7.18 (s, 2H, ArH), 7.45 (d, 2H, ArCH═CH, J = 16.7 Hz), 7.55 (d, 2H, ArCH═CH, J = 16.7 Hz). ^{13}C NMR ($CDCl_3$): δ 11.37, 11.46, 16.43, 16.60, 16.70, 16.74, 16.80, 26.12, 26.20, 26.24, 26.33, 34.89, 34.96, 35,08, 73.35, (OCH$_2$), 74.19 (OCH$_2$), 74.36 (OCH$_2$), 74.41 (OCH$_2$), 74.62 (OCH$_2$), 90.69 (C≡C), 91.99 (C≡C), 108.41, 109.85, 112.62, 114.22, 116.19, 116.24, 116.95, 117.19, 121.44, 124.10, 124.91, 127.86, 128.85, 150.28 (COCH$_2$), 150.53 (COCH$_2$), 152.64 (COCH$_2$), 153.52 (COCH$_2$), 154.19 (COCH$_2$). IR (KBr): ν (cm^{-1}) = 2958.1 (C−H sat), 2917.0 (C−H sat), 2873.4 (C−H sat), 2203.0 (C≡C). UV−vis (CH_2Cl_2): λ_{max} (ϵ) = 312 (33 000), 428 nm (99 000). MALDI TOF MS: 1371.5 [M]. Anal. Calcd for $C_{90}H_{130}O_{10}$: C, 78.79; H, 9.55. Found: C, 79.05; H, 9.53.

Acknowledgment. The Eindhoven-Mons collaboration is supported by the European Commission, under the RTN Network "Laminate". The work in Mons is partly supported by the Belgian Federal Government (Interuniversity Attraction Pole 4/11 on Supramolecular Chemistry and Supramolecular Catalysis) and the Belgian National Fund for Scientific Research (FNRS). The work at Arizona is partly supported by the National Science Foundation (CHE-0071889). The research of A.P.H.J.S. was made possible by a fellowship of the Royal Netherlands Academy of Arts and Sciences. David Beljonne is a research fellow of FNRS.

CM0109185